Static Strength Analysis of Pin-Loaded Lugs

J.C. Ekvall*
Lockheed-California Company, Burbank, California

A new method of analysis is presented for predicting the static strength of straight and tapered pin-loaded lugs. The method of analysis is applicable to both tension and shear bearing types of failure. It is shown that the bearing efficiency factor K_{BR} is uniquely related to the elastic tension stress concentration factor at the edge of the lug hole. Based on this relationship, a method of static strength analysis is developed that accounts for lug eccentricity and loading angle. The ratio of predicted load divided by test load for 243 lug tests made from 24 materials was 0.85–1.19, with a mean of 1.003. Based on these results, the method of analysis could be applied to other lug geometries if the elastic tension stress concentration factors are known.

Introduction

THE static strength methods of analyses for pin-loaded lugs have not changed since they were developed for axially loaded lugs in 1950[1] and for obliquely or transversely loaded lugs in 1953.[2] For axially loaded lugs, two analyses are required: one for tension failures across the net section and the other for shear tear-out failures between the pin and the end of the lug. The analyses make use of bearing efficiency factors, which are a function of lug geometry, and tension efficiency factors, which are a function of lug geometry and material properties. The allowable loads are predicted using these factors together with the lug geometry and the tensile ultimate strength of the lug material. Predictions are made without a knowledge of the stress distribution in the lug.

In Ref. 3, results were presented on the stress distribution in symmetrical straight lugs and symmetrical 45 deg tapered lugs based on finite element analyses. These results provided the opportunity to determine the relationship between lug static strength and peak tension stresses in the lug. In the present work, it was found that there is a unique relationship between the bearing efficiency factor and the stress concentration factor for the lug. Using this relationship, a method of static strength analysis was developed to account for lug eccentricity and loading angle.

Elastic Stress Concentration Factors for Pin-Loaded Lugs

In Ref. 3, the conventional two-dimensional (2-D) displacement finite element method was used to determine the distribution of stresses in a straight symmetric lug loaded in tension in the direction of the lug axis. Due to symmetry, only one-half of the lug was modeled. The lug and the pin were modeled with constant-strain triangular and quadrilateral elements. Spring elements were connected between the node points of the pin and the lug hole all around the periphery. The pin was assumed to have a stiffness three times greater than the lug. Additional analyses indicated the difference in stiffness between the pin and lug had a small effect on the peak tension stresses. The pin was assumed to fit in the lug hole with zero clearance and no frictional restraint. The contact area under loading was determined iteratively by assigning high stiffness to spring elements loaded in compression and very low stiffness (essentially zero) to spring elements loaded in tension.

The relationship between the elastic stress concentration factors K_{tb} and lug geometry determined from the results of the finite element analyses are plotted in Fig. 1. The elastic stress concentration factor is defined as the peak tangential tension stress at the edge of the lug hole divided by the average bearing stress σ_{BR}. As expected, the peak stress occurs at an angle of approximately 90 deg to the loading direction. The curve is drawn through the five analysis points using the equation given in Fig. 1. The elastic stress concentration factor given by the equation in Fig. 1 agrees with the computed points within 0.5%. Extrapolation using the equation beyond the range of computed values could introduce considerably larger errors.

Reference 3 also presents results of finite element analyses of 45 deg tapered lugs loaded at angles of 0, 45, and 90 deg. In these cases, the complete lug and pin were modeled using 72 triangular elements, 348 quadrilateral elements, 28 spring elements, 429 nodes, and 850 degrees of freedom. The stiffness of the pin material was assumed to be three times the stiffness of the lug material. The pin fit and connection between the pin and lug using springs was similar to that used for the analysis of the straight lugs.

The results of the finite analysis from Ref. 3 are plotted in Fig. 2. The elastic stress concentration for symmetrically loaded ($\theta = 0$ deg) tapered lugs as a function of taper angle β is given by[3]

$$K_{tb} = \left(2.75 - \frac{\beta}{135}\right)\left(\frac{2R_0}{D} - 1\right)^{-(0.675-\beta/1000)} \tag{1}$$

Equation (1) reduces to the equation given previously in Fig. 1 for $\beta = 0$ deg and the equation given in Fig. 2 for $\beta = 45$ deg.

Bearing Efficiency Factor

Applicable test data from Refs. 4-7 were evaluated to determine if there is a relation between the elastic stress concentration factor and lug ultimate strength. The bearing efficiency factor K_{BR} was calculated for each test result and plotted vs the elastic stress concentration factor K_{tb}. The bearing efficiency factor is defined by

$$K_{BR} = P/DtF_{tu} \tag{2}$$

where P is the lug failure load, D the lug hole diameter, t the lug thickness, and F_{tu} the lug material ultimate tensile strength.

Received July 23, 1985; revision received Nov. 25, 1985.

*Research and Development Engineer.

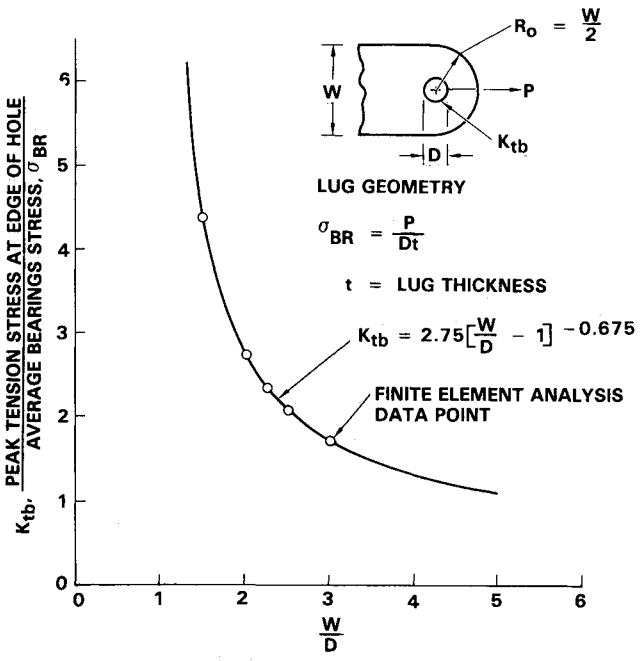

Fig. 1 Stress concentration factor for axially loaded straight lugs with $2R_0/W = 1.0$ (from Ref. 3).

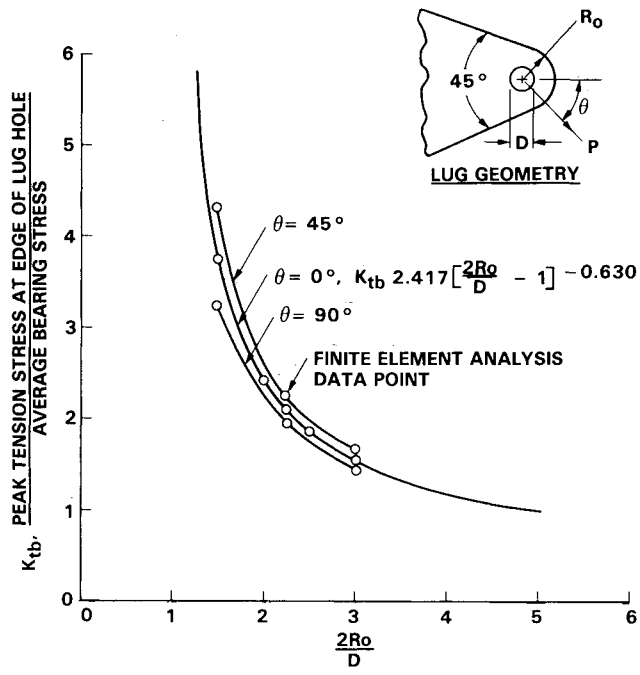

Fig. 2 Stress concentration factor for 45 deg tapered lugs loaded at angles of 0, 45, and 90 deg to the lug axis.

The test results plotted in Fig. 3 show there is a very good correlation between K_{BR} and K_{tb} with very little scatter about a best fit curve through the data points. The ultimate tensile strength for each material was taken as the average of two or three tensile tests conducted on specimens fabricated from the lug material. The applicable peak stress concentration factor for each lug was determined from Figs. 1 and 2. The test results include seven different materials, symmetric straight lugs loaded at 0 and 45 deg and symmetric tapered lugs loaded at 0, 45, and 90 deg. The data also include both tension and shear bearing modes of failure.

To further verify that there is a relationship between K_{BR} and K_{tb}, test data were evaluated for straight symmetric lugs loaded at an angle of 90 deg to the lug axis. The stress concentration factor is not available for this loading case. However, as shown previously in Fig. 1, the elastic stress concentration factor is related to the W/D ratio, i.e., the lug width divided by the hole diameter. Therefore, the bearing efficiency factor should also be related to W/D. Applicable data from Refs. 6-9, plotted in Fig. 4, shows there is a correlation between K_{BR} and W/D. A straight line through the data points, given by the equation in Fig. 4, provides a good fit to the data with very little scatter about the line. Two other lug materials, 300M and Ti-6A1-6V-2Sn, are included in the data shown in Fig. 4. These data further substantiate that the bearing efficiency factor is uniquely related to the elastic stress concentration factor.

If it is assumed that the relationship shown previously in Fig. 3 also applies to symmetrical straight lugs loaded at 90 deg, then the elastic stress concentration factor can be determined using the curve given in Fig. 4. This is done by determining the value of K_{BR} for a given value of W/D in Fig. 4 and then entering Fig. 3 with the K_{BR} value to determine K_{tb}. The value of K_{tb} determined in this manner is plotted in Fig. 5 together with the relationship for lugs loaded at 0 deg. The curve for the 90 deg loading case is slightly higher than for the 0 deg loading case for W/D values between 1.35 and 3.5. This relationship for straight lugs is somewhat different than for tapered lugs where the 90 deg loading case is slightly below the 0 deg loading case as shown previously in Fig. 2.

In Ref. 6, tests were conducted on straight lugs loaded at 0, 45, and 90 deg for five aluminum materials. These data indicate that the ultimate strength for lugs loaded at 45 deg

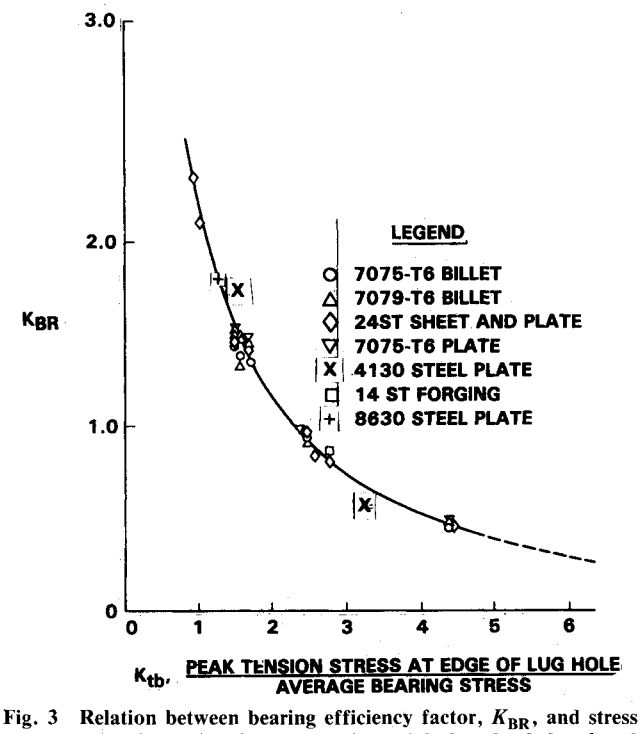

Fig. 3 Relation between bearing efficiency factor, K_{BR}, and stress concentration factor K_{tb} for symmetric straight lugs loaded at 0 and 45 deg and tapered lugs loaded at 0, 45, and 90 deg to the lug axis.

is between the ultimate strength for 0 and 90 deg angles of loading. Therefore, the elastic stress concentration factor for other loading angles can be determined by linear interpolation between the two curves given in Fig. 5.

Effect of Lug Eccentricity

Straight eccentric lugs are defined as lugs where the edge distance a is not equal to one-half the lug width. The direction and magnitude of the eccentricity effects the elastic stress concentration factor and, hence, the bearing efficiency factor. No information is available on the elastic stress con-

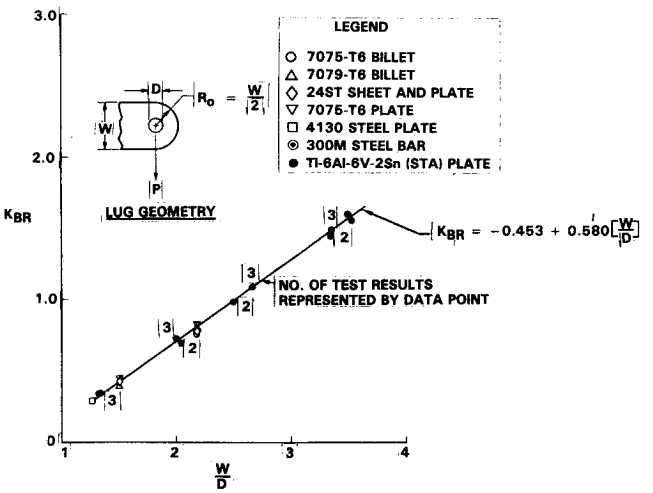

Fig. 4 Relation between bearing efficiency factor K_{BR} and lug geometry (W/D) for symmetric straight lugs loaded at 90 deg to the lug axis.

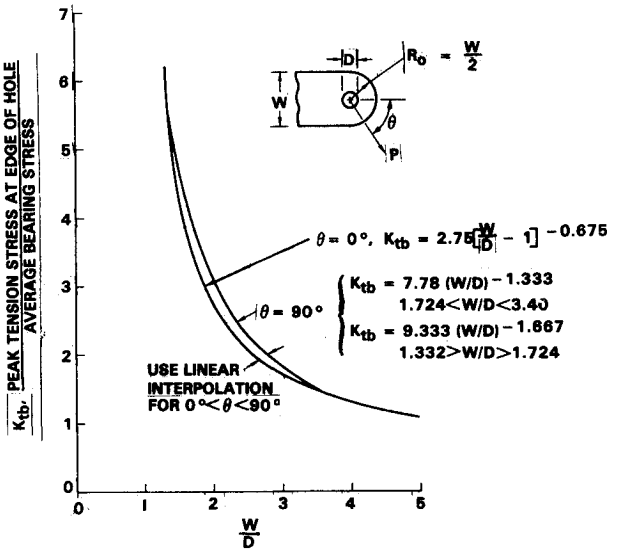

Fig. 5 Stress concentration factor for symmetric straight lugs loaded at 0-90 deg with respect to the lug axis.

centration factor for eccentric pin loaded lugs. However, there is a large amount of test data available for eccentric straight lugs loaded at angles of 0, 45, and 90 deg to the lug axis. These data were used to derive correction factors to account for the effect of lug eccentricity.

The data from Refs. 4-8 and 10 were used to develop correction factors for 0 and 90 deg loaded straight eccentric lugs. The value of K_{BR} obtained for each lug test result was used to determine the elastic stress concentration factor using Fig. 3. The corresponding K_{tb} value for a symmetric lug with the same value of W/D was then determined from Fig. 1. The ratio of the K_{tb} value obtained for the eccentric lug divided by the K_{tb} value of the reference symmetric lug was plotted vs the degree of eccentricity as given by the ratio $2a/W$. The results of the analysis for 0 and 90 deg lugs are shown in Fig. 6 together with a curve for $\theta = 45$ deg determined from evaluating data in Ref. 6. The scatter of the data about the curves drawn in Fig. 6 is about $\pm 12\%$.

Method of Static Strength Analysis

Based on the correlation between the elastic stress concentration factor and the bearing efficiency factor, a new method of analysis has been developed for predicting the static strength of pin loaded lugs. This method of analysis

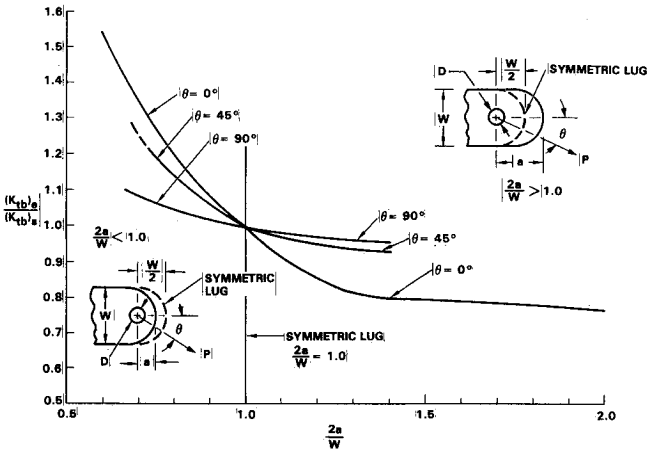

Fig. 6 Stress concentration correction factors for straight lugs loaded at angles of 0, 45, and 90 deg to the lug axis.

can be used to predict the ultimate strength of straight lugs and tapered lugs loaded at any loading angle between 0 and 90 deg to the lug axis, including the effect of lug eccentricity. It is possible that the method of analysis can also be applied to other lug geometries if the elastic stress concentration factor at the critical location is known. The method of analysis is applicable to both tension and shear bearing modes of failure, but does not account for localized bearing failure. The analysis procedure for straight and tapered lugs is outlined in the steps below.

Straight Lugs

Given lug geometry a, W, D, t; material properties F_{tu} (use minimum strength with respect to gain direction) and loading angle θ:

1) Compute W/D and $2a/W$.

2) Enter Fig. 5 with W/D to determine the value of the elastic stress concentration factor $(K_{tb})_s$ for a symmetric lug. Use linear interpolation between curves for loading angles other than 0 or 90 deg.

3) Enter Fig. 6 with $2a/W$ and θ to determine the eccentricity correction factor $(K_{tb})_e/(K_{tb})_s$.

4) Compute $(K_{tb})_e$ by multiplying the values obtained from step 2 by the values obtained from step 3, i.e.;

$$(K_{tb})_e = \frac{(K_{tb})_e}{(K_{tb})_s} \times (K_{tb})_s$$

5) Enter Fig. 3 with $(K_{tb})_e = K_{tb}$ to obtain K_{BR}.

6) Compute the predicted failure load by

$$P = D \cdot t \cdot K_{BR} \cdot F_{tu}$$

Tapered Lugs

Given lug geometry a, R_0, D, t, and β where R_0 is the shortest distance from the center of the lug hole to the taper angle; material properties F_{tu} (use minimum strength with respect to grain direction) and loading angle θ:

1) Compute $2R_0/D$ and a/R_0.

2a) For $\beta = 45$ deg, enter Fig. 2 with θ and $2R_0/D$ to obtain $(K_{tb})_s$.

2b) For $0 < \beta < 45$ deg and $\theta = 0$ deg, compute $(K_{tb})_s$ from

$$(K_{tb})_s = \left(2.75 - \frac{\beta}{135}\right)\left(\frac{2R_0}{D} - 1\right)^{-(0.675 - \beta/1000)}$$

2c) For cases not covered by step 2a or 2b, compute the following:

i) Enter Fig. 5 with $2R_0/D = W/D$ to obtain $(K_{tb})_\theta$ for a straight symmetric lug loaded at the angle θ.

ii) For $\beta = 45$ deg and $\theta = 0$ deg, calculate $(K_{tb})_{0°}$ from

$$(K_{tb})_{0°} = 2.417\left(\frac{2R_0}{D} - 1\right)^{-0.630}$$

iii) For $\beta = 45$ deg and $\theta \neq 0$ deg, calculate $(K_{tb})_\theta / (K_{tb})_{0°}$ from

$$K_{tb\theta}/(K_{tb})_{0°} = 1 + 6.33 \times 10^{-3}\theta - 8.15 \times 10^{-5}\theta^2$$

where θ is expressed in degrees.

iv) Compute $(K_{tb})_\theta$ by multiplying the value of $(K_{tb})_\theta/(K_{tb})_{0°}$ from step iii by the value of $(K_{tb})_{0°}$ from step ii. The $(K_{tb})_\theta$ values obtained by this procedure for $\theta = 45$ and 90 deg are within $\pm 5\%$ of the values given in Ref. 3.

v) For $0 < \beta < 45$ deg, use linear interpolation between the value of $(K_{tb})_\theta$ obtained from step i and $(K_{tb})_\theta$ obtained from step iv to obtain the value of $(K_{tb})_s$.

3) If $a/R_0 \neq 1.0$, let $a/R_0 = 2a/W$. It is assumed that the eccentricity correction factor for tapered lugs is the same as for straight lugs. Obtain the eccentricity correction factor $(K_{tb})_e/(K_{tb})_s$ from Fig. 6.

4) Compute $(K_{tb})_e$ by multiplying the value of $(K_{tb})_s$ obtained from step 2a, 2b, or 2c by the eccentricity correction factor obtained from step 3.

5) Enter Fig. 3 with $(K_{tb})_e = K_{tb}$ to obtain K_{BR}.

6) Compute the predicted failure load by

$$P = D \cdot t \cdot K_{BR} \cdot F_{tu}$$

Correlation of Analysis and Lug Test Data

The test data from Refs. 4-14 were analyzed using the methods of analysis given previously. Test data from Refs. 11-14, which were not used to develop the methods of analysis, were included in the correlations. The data includes 263 tests conducted on 25 different materials with the tensile material properties given in Table 1. The distribution of the data with respect to the type of lug and loading angle is given in Table 2. The range of parameters covered by the tests were lug hole diameters of 0.25-2.85 in., material thicknesses of 0.049-2.125 in., D/t ratios of 0.76-10.2, W/D ratios of 1.33-4.5, and $2a/W$ values of 0.73-2.0.

The probability distribution of test load to predicted load ratios for 224 predictions (243 tests) is shown in Fig. 7. The 20 results for material 1 in Table 2 were not included because of the large scatter in tensile strength properties. These

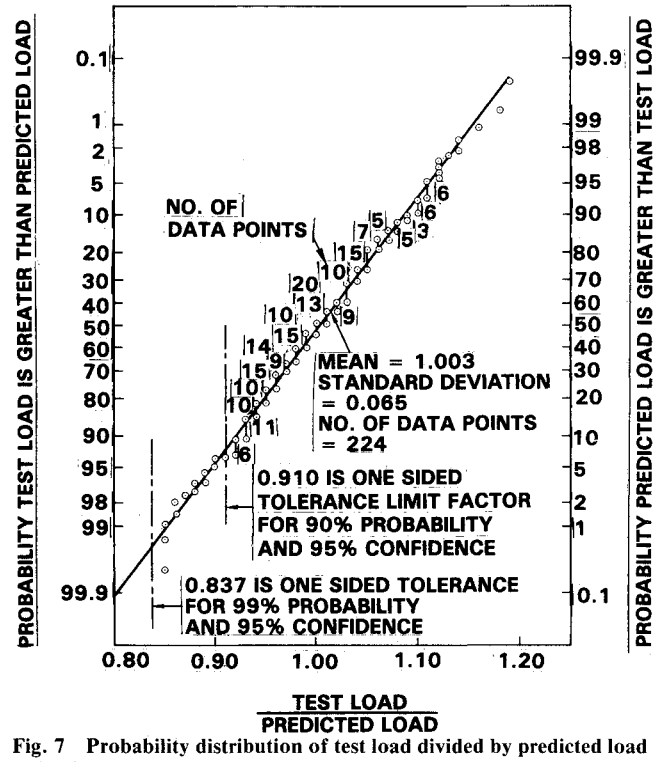

Fig. 7 Probability distribution of test load divided by predicted load ratios for lug ultimate strength.

Table 1 Properties of materials used for tests conducted on various lugs

Item	Material	Ultimate tensile strength, psi	Tensile yield strength, psi	Elongation, %	No. of tests[e]
1	356-T6 sand casting	17,560-26,100	—	—[a]	20
2	7075-T6 hand-forged billet	76,860	64,230	6.83[b]	20
3	7079-T6 billet	76,450	63,000	8.20[b]	19
4	2024-T4 plate	70,220	48,890	18.83[c]	21
5	7075-T6 plate	82,510	72,520	12.5[c]	20
6	0.250 in. 8630 steel plate	131,300	101,400	8.0[c]	3
7	0.250 in. 24S-TO aluminum plate	65,300	39,900	19.5[c]	4
8	0.072 in. 24S-TO aluminum sheet	67,700	42,400	20[c]	1
9	0.051 in. 24S-TO aluminum sheet	65,400	46,400	20[c]	1
10	195-T6 aluminum casting	21,500	18,200	0.9[c]	2
11	FS1H magnesium sheet	47,800	40,000	18[c]	1
12	0.125 in. 24ST Al clad sheet	66,880	49,680	18[c]	5
13	14ST forging	68,500	59,050	14[c]	5
14	0.250 in. 4130 steel plate	171,000	161,600	13.2[c]	5
15	75ST plate	83,700	72,600	—	4
16	Steel plate	192,000	181,000	—	1
17	Steel plate	109,800	88,600	—	1
18	Ti-6Al-6V-2Sn (STA) plate	174,700	168,300	16.5[c]	32
19	24ST aluminum plate	73,000	48,900	20.7[c]	6
20	4130 steel plate	98,130	75,600	20.0[c]	11
21	300M steel bar	283,500	241,500	11.2	6
22	Ti-6Al-6V-2Sn forging[d]	150,000	140,000	10	3
23	7075-T73 plate	73,600	64,100	8.2	3
24	Ti-6Al-4V plate	144,800	136,400	—	68
25	24ST aluminum plate	65,250	49,400	8.0	1
				Total	263

[a]Strain < 0.2%. [b]1 in. gage length. [c]2 in. gage length. [d]MIL-HDBK-5D "S" values. [e]Includes only tension and shear-bearing failures.

Table 2 Summary of test data by type of lug and loading angle

Type of lug	Load angle with respect to lug axis 0 deg	18 deg	30 deg	45 deg	90 deg	No. of tests
Straight lugs						
$2a/W<1.0$	34			5	15	54
$2a/W=1.0$	54	3	3	16	35	111
$2a/W>1.0$	53			7	13	73
Tapered lug						
30 deg taper[a]	1					1
45 deg taper[a]	10			5	9	24
No. of tests	152	3	3	33	72	263

[a]Approximate angles of taper.

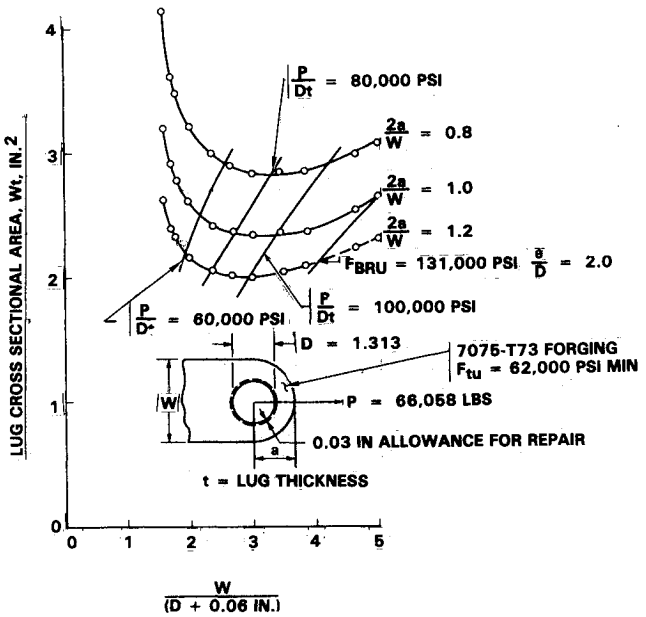

Fig. 8 Effect of varying lug geometry on cross sectional area of example aluminum lug.

results are discussed below. Also, materials 2-4 had 19 duplicate tests that were averaged to correlate with one prediction. The results fit close to a normal probability distribution with a mean of 1.003 and a standard deviation of 0.065. If a multiplying factor of 0.91 is applied to the predicted load, one can state that at least 90% of the test values are expected to exceed the predicted values with a confidence of 95%. For a multiplying factor of 0.837, a similar statement can be made for a 99% probability and 95% confidence level. These correlations are based on the use of material properties determined from the average of tensile tests conducted on specimens fabricated from the lug material.

The 356-T6 sand casting lug test data were analyzed separately. As one would expect, this material has a wide scatter in tensile properties, probably due to a variation in the defect size at critical locations in the test specimens. There was also a large scatter in the lug test data for this material. Rather than predict load, the data was analyzed to predict the tensile ultimate strength using the test load and the methods of analysis given above. One test result failed at 45% of the predicted load. The other 19 tests indicated tensile ultimate strengths ranging from a low of 17,570 psi to a high of 30,340 psi, with a mean of 24,600 psi. The tensile strength properties obtained from three tests varied between 17,560 and 26,100 psi, with a mean of 22,590 psi. Therefore, the lug tests results indicate about the same variation in tensile properties as the results from three tensile coupons. Based on the average values, the test loads were about 15% higher than the predicted loads.

Conclusions

The method of analysis correlates well with test results for both tension and shear bearing types of failure. Therefore, only one analysis needs to be made to account for both failure types. The reason the analysis is applicable to both failures is because both initiate at the edge of the hole where the peak tensile stress is the highest. The mode of failure depends on the material properties and lug geometry. Materials with low fracture toughness generally fail in a tension mode with a flat fracture across the width of the lug. Materials with high ductility and fracture toughness can fail either in a tension or shear bearing failure mode, depending on lug geometry. For narrow lugs, the fracture could propagate across the width of the lug in a tension failure mode. For wider lugs, the crack would initiate along a shear plane at the edge of the hole and propagate to failure at an angle to the lug axis in a shear bearing failure mode.

As shown previously in Figs. 3 and 4, the bearing efficiency factor K_{BR} is uniquely related to the elastic stress concentration factor for all materials for which there is data. Why would one curve fit all materials? First, the theoretical distribution of stress around the lug hole is nearly the same for all materials with the same elastic stress concentration factor because differences in moduli between the lug and the pin have a small effect on the elastic stress concentration factor. Plasticity affects only a small area of material in the vicinity of the stress concentration; therefore, one would expect the distribution of stress at failure for the various materials to be related to the elastic stress distribution and be proportional to the material's ultimate tensile strength.

Another mode of failure that must be considered is localized bearing failure at the lug hole. A number of bearing failures occurred in the tests that were reported in Refs. 5 and 8. These results were not included in this evaluation. In practice, lugs usually have bushings or bearings that must be lubricated periodically. The bearing pressures are usually limited to values well below the bearing strength of the material to prevent excessive wear and to keep the lubricant from squeezing out. While limiting the bearing pressures prevents bearing failures, it affects the size and shape of the lug for the design load conditions as discussed below.

The lug static strength is directly related to the material ultimate tensile strength, as indicated by the equations given earlier. In all of the lug tests evaluated, the tensile strength was determined in only one grain direction, which usually was not identified. However, all of the materials listed in Table 1 would have a small difference in tensile properties with respect to grain direction. If the tensile properties vary with grain direction, the minimum tensile properties should be used.

All the lug tests evaluated were conducted with solid steel pins. In Ref. 10, some tests were conducted using pins with Rockwell C hardness values of 18-46.5. Only the tests with the maximum strength pins in Ref. 10 were used. None of the pins failed in the tests, but the minimum strength pins were severely deformed during the tests. The effect of the variation in bending deformation of the pin only reduced the ultimate strength a maximum of 14% for the seven groups of lug tests. Therefore, the effect of pin deflection does not appear to have a large effect on the strength of lugs made from materials with good ductility.

Reference 8 contained fifteen test results of lugs with square ends. These lugs were analyzed as though they were straight lugs with an outside radius R_0 equal to one-half the lug width. The ratios of the test load to the predicted load for these tests were 0.92-1.12 with a mean of 1.002. Therefore, the effect of extra material in the corners of a lug has a small effect on the static strength.

An aluminum lug on the L-1011 main landing gear was analyzed to determine the effect of varying lug geometry on the lug structural weight as indicated by the cross-sectional area Wt. For this analysis, it was assumed that there are no limitations on lug dimensions. The lug was made from 7075-T73 aluminum forging with a minimum tensile strength of 62,000 psi, a pin diameter of 1.313 in., and an allowance of 0.06 in. on the diameter for in-service repairs. The pin diameter was held constant since analysis indicated that varying the pin diameter had no effect on the required cross-sectional area. The width and thickness were varied to support an axial load of 66,058 lb. The analysis was also conducted for three ratios of $2a/W$ to show the effect of eccentricity on the required cross-sectional area.

The results of the analysis are summarized in Fig. 8. The minimum cross-sectional area is obtained for a W/D ratio of approximately 3.0 for all values of $2a/W$. However, the area does not change much for W/D ratios between 2 and 4. W/D ratios above 4 are limited by the ultimate bearing strength of the material. Placing limitations on the allowable ultimate bearing stress below about 90,000 psi forces the design to lower W/D ratios with some increase in cross-sectional area. The required cross-sectional area can be reduced further by increasing the end distance a until the F_{BRU} curve intersects a $2a/W$ curve at the minimum cross-sectional area. This may be an effective way to reduce the weight of a clevis, but may not be practical for the lug because the clevis would have to be longer.

In conclusion, the static strength of lugs can be accurately predicted using the methods of analysis presented here. The methods can be used as an aid in designing lugs for minimum weight. The only material properties required for the analysis are the ultimate tensile strength and bearing strength. Of course, many other factors in addition to static strength must be considered in designing lugs. Serviceability of the lugs is very important and includes consideration of fatigue, damage tolerance, corrosion, wear, and allowance for repair in service. Also, appropriate fitting factors, casting factors, and permissible minimum margins of safety must be considered in the design of lugs. However, these can be accounted for by designing the lugs for the increased loads that include the appropriate factors.

References

[1]Cozzone, F.P., Melcon, M.A., and Hoblit, F.M., "Analysis of Lugs and Shear Pins Made of Aluminum or Steel Alloys," *Product Engineering*, Vol. 21, No. 5, May 1950, pp. 113-117.

[2]Melcon, M.A. and Hoblit, F.M., "Development in the Analysis of Lugs and Shear Pins," *Product Engineering*, Vol. 24, No. 6, June 1953, pp. 160-170.

[3]Katherisan, K., Hsu, T.M., and Brussat, T.R., "Advanced Life Analysis Methods Volume II—Crack Growth Analysis Methods for Attachment Lugs," AFWAL-TR-84-3080, Sept. 1984.

[4]Kastan, H. and Sangster, W., "Tests of Eccentric Lugs," Lockheed-California Co., Burbank, CA, Rept. 2045, Nov. 1940.

[5]Grebe, H.W., "Tests of Aluminum, Steel and Magnesium Lugs," Lockheed Rept. 6042, Jan. 1947.

[6]Norair Div., Northrop Corp., unpublished lug data, Jan. 1960.

[7]Bonell, W.H., "Static Tests of Lugs with Transverse Loads," Lockheed-California Co., Burbank, CA, Rept. 6723, Oct. 1948.

[8]Snider, H.L. and Stemme, H.W., "Design and Lug Strength Testing for Diffusion Bonded Ti-6A1-6V-2Sn," Lockheed-Georgia Co., Marietta, GA, Rept. SMN 266, June 1969.

[9]Webber, M.D., "S-3A Static Lug Test, Landing Gear Strut Attachments," Lockheed-California Co., Burbank, CA, Rept. 24164, Dec. 1970.

[10]Addison, J.V., "Static Tests of Pin Bending in Lugs," Lockheed-California Co., Burbank, CA, Rept. 7394, April 1950.

[11]Masgrove, M.D. and Mortensen, R.E., "Development of Titanium Structural Element Allowables for the Boeing SST," 11th AIAA/ASME/SDM Conference, Denver, CO, April 1970.

[12]Webber, M.D., "S-3A Static Lug Test, Arresting Gear Attachment Fittings," Lockheed-California Co., Burbank, CA, Rept. 24168, Dec. 1970.

[13]Webber, M.D., "S-3A Static Lug Test Main Landing Gear Attachment Fittings," Lockheed-California Co., Burbank, CA, Rept. 24169, Dec. 1970.

[14]Fish, C.H., "Static Tests of Corroded and Uncorroded Drag Link Rib Lugs," Lockheed-California Co., Burbank, CA, Rept. 6244, Sept. 1947.